



# Stress-induced activation of brown adipose tissue prevents obesity in conditions of low adaptive thermogenesis

Maria Razzoli<sup>1,8</sup>, Andrea Frontini<sup>2,8</sup>, Allison Gurney<sup>1,8</sup>, Eleonora Mondini<sup>2</sup>, Cankut Cubuk<sup>3</sup>, Liora S. Katz<sup>4</sup>, Cheryl Cero<sup>1</sup>, Patrick J. Bolan<sup>5</sup>, Joaquin Dopazo<sup>3</sup>, Antonio Vidal-Puig<sup>6,7</sup>, Saverio Cinti<sup>2</sup>, Alessandro Bartolomucci<sup>1,\*</sup>

## ABSTRACT

**Background:** Stress-associated conditions such as psychoemotional reactivity and depression have been paradoxically linked to either weight gain or weight loss. This bi-directional effect of stress is not understood at the functional level. Here we tested the hypothesis that pre-stress level of adaptive thermogenesis and brown adipose tissue (BAT) functions explain the vulnerability or resilience to stress-induced obesity.

**Methods:** We used wt and triple  $\beta_1, \beta_2, \beta_3$ -Adrenergic Receptors knockout ( $\beta$ -less) mice exposed to a model of chronic subordination stress (CSS) at either room temperature (22 °C) or murine thermoneutrality (30 °C). A combined behavioral, physiological, molecular, and immunohistochemical analysis was conducted to determine stress-induced modulation of energy balance and BAT structure and function. Immortalized brown adipocytes were used for in vitro assays.

**Results:** Departing from our initial observation that  $\beta$ ARs are dispensable for cold-induced BAT browning, we demonstrated that under physiological conditions promoting low adaptive thermogenesis and BAT activity (e.g. thermoneutrality or genetic deletion of the  $\beta$ ARs), exposure to CSS acted as a stimulus for BAT activation and thermogenesis, resulting in resistance to diet-induced obesity despite the presence of hyperphagia. Conversely, in wt mice acclimatized to room temperature, and therefore characterized by sustained BAT function, exposure to CSS increased vulnerability to obesity. Exposure to CSS enhanced the sympathetic innervation of BAT in wt acclimatized to thermoneutrality and in  $\beta$ -less mice. Despite increased sympathetic innervation suggesting adrenergic-mediated browning, norepinephrine did not promote browning in  $\beta$ ARs knockout brown adipocytes, which led us to identify an alternative sympathetic/brown adipocytes purinergic pathway in the BAT. This pathway is downregulated under conditions of low adaptive thermogenesis requirements, is induced by stress, and elicits activation of UCP1 in wt and  $\beta$ -less brown adipocytes. Importantly, this purinergic pathway is conserved in human BAT.

**Conclusion:** Our findings demonstrate that thermogenesis and BAT function are determinant of the resilience or vulnerability to stress-induced obesity. Our data support a model in which adrenergic and purinergic pathways exert complementary/synergistic functions in BAT, thus suggesting an alternative to  $\beta$ ARs agonists for the activation of human BAT.

© 2015 The Authors. Published by Elsevier GmbH. This is an open access article under the CC BY-NC-ND license (<http://creativecommons.org/licenses/by-nc-nd/4.0/>).

**Keywords** Subordinate; Energy expenditure; UCP1; P2RX5; Purinergic

## 1. INTRODUCTION

Metabolic diseases (e.g. obesity, type 2 diabetes) are rising exponentially to a pandemic level. A substantial number of obese individuals manifest psychiatric comorbidity, experience stressful life events, and typically report more medical complaints and poorer quality of life [1,2]. Stress and negative affect are increasingly recognized as risk factors for eating disorders and obesity [3,4].

Despite major advances in our understanding of the signaling pathways linking food intake and energy homeostasis [5,6], we possess very few therapeutic answers to the obesity epidemic [7,8]. Brown adipose tissue (BAT), a thermogenic organ likely to play a major role in energy balance, obesity and diabetes [9,10], is emerging as a novel target for anti-obesity and diabetes pharmacotherapies. The mechanisms of BAT activation are increasingly investigated after the (re) discovery of functional BAT in adult humans [11–14] and the

<sup>1</sup>Department of Integrative Biology and Physiology, University of Minnesota, Minneapolis, MN 55455, USA <sup>2</sup>Department of Experimental and Clinical Medicine, Center for Obesity, Università Politecnica delle Marche, Ancona 60020, Italy <sup>3</sup>Computational Genomics Department, Centro de Investigación Príncipe Felipe, C/ Eduardo Primo Yufera 3, 46012 Valencia, Spain <sup>4</sup>National Institute of Diabetes and Digestive and Kidney Diseases, National Institutes of Health, Bethesda, MD 20892, USA <sup>5</sup>Department of Radiology and Center for Magnetic Resonance Research, University of Minnesota, MN 55455, USA <sup>6</sup>University of Cambridge Metabolic Research Laboratories, Cambridge CB2 0QQ, UK <sup>7</sup>Wellcome Trust Sanger Institute, Wellcome Trust Genome Campus, Hinxton, Cambridge, CB10 1SA, UK

<sup>8</sup> Maria Razzoli, Andrea Frontini and Allison Gurney contributed equally to this work.

\*Corresponding author. Department of Integrative Biology and Physiology, University of Minnesota, 2231 6th St. SE, Minneapolis, MN 55455, USA. Tel.: +1 612 626 7006; fax: +1 612 301 1229. E-mail: [abartolo@umn.edu](mailto:abartolo@umn.edu) (A. Bartolomucci).

Received September 26, 2015 • Revision received October 9, 2015 • Accepted October 13, 2015 • Available online 11 November 2015

<http://dx.doi.org/10.1016/j.molmet.2015.10.005>

identification of beige adipocytes [15–17]. It is accepted that the thermogenic function of brown adipocytes is regulated by sympathetic nervous system release of norepinephrine that, through  $\beta$  adrenergic receptors ( $\beta$ -ARs) induced lipolysis, culminates in UCP1 (uncoupling protein 1) activation and heat generation [9,18–20].  $\beta$ ARs agonists are powerful activators of BAT in mice and humans [21]. However, their relative lack of selectivity resulting in cardiovascular activation has refocused the therapeutic interest in identifying alternative non-adrenergic mechanisms of BAT activation [7,8,10]. Cold-elicited increase in brown/beige adipocyte activity in humans seems stronger compared to pharmacological stimulation with  $\beta$ ARs agonists [22–25], thus suggesting a contribution of additional mediators other than NE/ $\beta$ AR to BAT mediated thermogenesis. Notably, humans experience only a modest basal activation of BAT as a result of their high body weight/surface area and predominant exposure to thermoneutral comfort zone, which results in low sympathetic tone to fat pads and low norepinephrine/ $\beta$ AR signaling compared to rodents [9,26,27]. Accordingly, identifying an alternative activator of the thermogenic program that can be activated under conditions of low BAT activity and/or a  $\beta$ ARs-independent mechanism of browning is of enormous translational relevance to generate therapies without sympathomimetic-like side effects. In this study, departing from the original observation that  $\beta$ -ARs are dispensable for cold-induced BAT browning, we demonstrated that resilience to chronic subordination stress-induced obesity [28] is determined by a pre-stress state of low adaptive thermogenesis and BAT function, overall providing a functional explanation for the biphasic effect of chronic stress on energy balance [e.g. 29,30]. Furthermore, we identified a sympathetic/brown adipocyte purinergic pathway in mice that is downregulated at thermoneutrality, which is induced by subordination stress and that mediates browning in brown adipocytes. Importantly, we showed that this pathway is conserved in human BAT.

## 2. EXPERIMENTAL PROCEDURES

### 2.1. Animals and diet

$\beta$ 1, $\beta$ 2, $\beta$ 3 adrenergic receptor knockout ( $\beta$ -less) mice and their specific wt background strain were previously developed and described by Bachman et al. [19]. Mice were maintained in a fully controlled animal facility (12:12 h light:dark cycle at  $22 \pm 2$  °C). Homozygous breeding pairs were established and pups were weaned in groups of same-sex and same-genotype siblings. Animal experiments were conducted at University of Minnesota (USA) and approved by the Institutional Animal Care and Use Committee, University of Minnesota. Mice were fed a standard (D12405B, Research Diet 3.85 kcal/g, 10% kcal from fat) or a high fat (D12451, Research Diet, 4.73 kcal/g, 45% kcal from fat).

### 2.2. Overview of the experimental procedures

Experimental male mice were transferred from the animal facility to an adjacent fully controlled environmental room and housed in a 12:12 h light:dark cycle at  $14 \pm 2$  °C,  $22 \pm 2$  °C or  $30 \pm 2$  °C (wt only) according to the experimental conditions detailed below. Mice were allowed one month to acclimate to  $14 \pm 2$  °C or  $30 \pm 2$  °C before performing any experimental procedure.

#### 2.2.1. Mild cold experiment in $\beta$ -less mice

Mice acclimated for one month to  $14$  °C were then tested in the indirect calorimetry maintained at  $14$  °C for the entire duration of the recording. Mice were then allowed 4 days recovery from the calorimetry assessment, after which they were fasted overnight to then

undergo a glucose tolerance test. Mice were sacrificed 4 days later at 9 AM.

#### 2.2.2. Chronic subordination stress in wt mice acclimatized to $22$ °C or $30$ °C and in $\beta$ -less acclimatized to $22$ °C

For all the social stress experiments, the experimental phase consisted of a baseline phase of 5 days, during which all mice received standard diet, and of a stress phase during which all mice received standard diet on the first week of stress and high fat diet for the following weeks according to our published methods [28,31,32]. This enables the establishment of the social hierarchy without any confounding factor due to metabolic effect of the diet. Body weight and food intake were monitored regularly throughout the experimental procedure. Mice underwent body composition analysis once during baseline, and once during the last week of stress prior to the indirect calorimetry assessment (calorimetry maintained at the respective housing temperature for the entire duration of the recording). After 4 days of recovery from indirect calorimetry, all mice underwent an overnight fasting followed by the measurement of their blood glucose levels. Mice were sacrificed 4 days later at 9 AM.

#### 2.2.3. Behavioral experiments

A separate subset of wt and  $\beta$ -less mice acclimatized to  $22$  °C was used and subjected to same chronic subordination stress general procedure described above. In addition, locomotor activity was measured in home-cage throughout the duration of the procedure. During the last week of stress, mice were given overnight a two-bottle choice for sucrose preference test, and, 3 days later, they were tested in the forced swim test. Mice were sacrificed immediately after the completion of the forced swim test to collect blood and allow for corticosterone analysis in response to heterotypical stress.

### 2.3. Chronic subordination stress

The stress protocol was conducted as previously described [28,31,32]. Briefly individual  $\beta$ -less and wt mice were transferred as intruder in the home cage of a CD1 aggressive dominant. Dominant and intruder mice were allowed to freely interact for a maximum of 10 min. All wt and  $\beta$ -less mice included in the study were subordinated by CD1 males. After the interaction, resident and intruder mice were separated by a perforated partition, which allowed continuous sensory contact but no physical interaction. During the social interaction, offensive behaviors of the animals were manually recorded and mice social status was determined as previously established and detailed [28,31,32]. The partition was removed daily (between 8:30 and 9:30 AM), for a maximum of 10 min. Only dyads that reliably showed a stable dominant/subordinate hierarchy and in which the subordinate showed no attack after day 4 were included in the study. Age and weight-matched mice, housed in groups of 3 siblings, were included as the control group according to our standard validated protocol [28,31]. Animals included in the stress group were sibling of the animals used as controls.

### 2.4. Behavioral and endocrine assessment of depression-like behavior

#### 2.4.1. Home-cage activity

Locomotor activity was determined throughout the experiments in subordinate mice by means of an automated system that used small passive infrared sensors positioned on the top of each cage (ActiMeter, TechnoSmart, Rome, Italy) [31].

#### 2.4.1. Sucrose preference test

Mice were given a free choice between two bottles, one with 2.5% sucrose solution and another with tap water in the housing cage. The beginning of the test started with the onset of the dark (active) phase of the animals' cycle and ended 12 h later. The consumption in water, sucrose solution and total intake of liquids is estimated simultaneously by weighing the bottles. The preference for sucrose was calculated as a percentage of the consumed sucrose solution from the total amount of liquid drunk by the formula:

$$\text{Sucrose Preference} = \frac{\text{Volume (Sucrose solution)}}{\text{Volume (Sucrose solution)} + \text{Volume (Water)}} \times 100.$$

To minimize the possible effect of novelty avoidance and to control for inter-individual variability, all mice were exposed to the procedure for the first time during baseline.

#### 2.4.2. Forced swim test (FST)

Mice were individually forced to swim in an open cylindrical glass container (diameter 10 cm, height 25 cm), containing 10 cm of water at  $25 \pm 1$  °C, for 6 min. The water was changed before the introduction of each animal. Mouse behavior was video-recorded by a video-camera placed in front of the glass cylinders. A trained observer blind to mouse experimental group scored videotapes recorded using The Observer XT 7.0 software (Noldus Information Technology, The Netherlands). The duration (s) of immobility (floating, defined as minimal activity required for the mouse to keep its head above water level) was scored from videotapes during the last 4 min of the 6 min test according to established methods. Mice were sacrificed at the end of the FST to determine plasma concentration of corticosterone in response to a heterotypic stress.

#### 2.5. Plasma analysis

Mice were euthanized by decapitation following brief CO<sub>2</sub> exposure. Mice were sacrificed within 3 min after an experimenter entered the animal room. Trunk blood was collected in EDTA coated tubes (Sarstedt) and spun at  $1,500 \times g$  for 10 min at 4 °C for plasma separation. Corticosterone was measured by RIA as previously described [33]. Other hormones were analyzed using Bio-Plex ProTM mouse assay kits and measured with Bio-Plex1 system (Bio-Rad Laboratories, Inc., USA) following manufacturer's protocol. Obtained fluorescent intensities for each hormone were analyzed using Masterplex software.

#### 2.6. Indirect calorimetry and body composition

Oxygen consumption (VO<sub>2</sub>) and carbon dioxide production (VCO<sub>2</sub>) were measured using the Oxymax Comprehensive Lab Animal Monitoring System (Columbus Instruments). Energy expenditure was calculated with the formula provided by the manufacturer, expressed as Kcal/h and analyzed with body weight as continuous predictors in an ANCOVA model [34]. Body composition was measured with Echo MRI 3-in-1 (Echo Medical System).

#### 2.7. 7-Tesla magnetic resonance imaging

Mice were sacrificed and placed in a 50 mL centrifuge tube prior to imaging on a 7T Siemens MR system (Erlangen, Germany) using a single-channel birdcage coil designed for whole-mouse imaging (Virtumed LLC, Minneapolis). Images were acquired with a 3D CISS (constructive interference in steady state) sequence, with an imaging matrix of  $280 \times 640 \times 144$ , nominal resolution  $188 \times 188 \times 190$  μm, flip angle 50°, TR/TE = 7.8/3.4 ms, readout bandwidth 326 Hz/pixel, 7/8 partial Fourier, and a total acquisition time of 8 min 35 s. The

interscapular BAT region was identified using a combination of anatomical prior knowledge and strong contrast with the subcutaneous visceral adipose tissue on the images we acquired. The CISS method we used is a standard method provided by the MRI vendor that is commonly used for inner ear imaging and other high-resolution applications [35–37]. The CISS technique provides very high resolution and sensitivity to the contrast mechanisms known to differ between murine BAT and WAT. Several papers using quantitative water-fat imaging techniques have shown that murine BAT has a lower T2\* (transverse NMR relaxation times) and fat content compared to WAT [35–37].

#### 2.8. Quantitative real-time polymerase chain reaction, microarray expression and pathway analysis

TRIzol reagent (Life Technologies) was used to isolate total RNA from frozen tissue. iScript cDNA synthesis kit (Bio-Rad, Hercules, CA) was used to synthesize 4000 ng of RNA. Gene transcription was measured with iQ SYBR Green supermix (Bio-Rad) in duplicate for target genes (Table S3 lists primer information) on a CFX96 Real-time PCR system (Bio-Rad). The best keeper was generated using 2–5 reference genes [38] and used to normalize target gene values according to the comparative threshold  $\Delta\text{CT}$ . Gene expression data is presented as normalized linear-transformed values ( $2^{-\Delta\text{CT}}$ ) and normalized over expression levels of controls.

Total RNA was isolated with the RNeasy mini elute kit (Qiagen) following manufacturer's instructions. All RNA samples had RNA quality scores above 7, as assessed with the LCGX system (Caliper Life Sciences). RNA was biotinylated and amplified using the Illumina TotalPrep RNA Amplification Kit (Life Technologies) for hybridization with the MouseWG-6 v2.0 Expression BeadChip Kit (Illumina) and scanned on the Illumina iScan at the Genomics Center, University of Minnesota. Microarray raw data files were normalized with R package "limma", using the "rank invariant" method. Normalized and log<sub>2</sub> transformed data are further analyzed in the Babelomics suite [39]. Firstly, differential expression between the compared conditions was carried out by using a two-tailed Fisher exact test. Functional enrichment by Gene Set Enrichment Analysis was carried out over the list of genes, arranged by differential expression, using FatiScan [40]. Redundant GO terms were removed by means of the program REVIGO, with parameters: similarity of 0.4, based on adjusted p-value (obtained from FatiScan), SimRel for semantic similarity and Mus musculus for GO terms.

#### 2.9. Western blot

Protein lysates were obtained by homogenizing tissue with a tissue homogenizer (Pracellys) in lysis buffer (25 mM HEPES, 150 mM NaCl, 5 mM EDTA, 5 mM EGTA, 5 mM glycerophosphate, 0.9% triton x-100, 0.1% NP-40, 5 mM sodium pyrophosphate, 1% glycerol, 1 mM PMSF, 20 μg/ml aprotinin, 1 μg/ml leupeptin, 0.5 mM sodium vanadate and 1 tablet PhosSTOP [Roche]). DNA content (200 ng total DNA) was used to load tissue lysates as a method of normalizing based on cell number. Lysates were resolved on 12% acrylamide gels, transferred to PVDF membranes, and probed overnight with primary UCP1 (Abcam ab10983, 1:1000 dilution). IRDye680LT donkey anti-rabbit (Li-Cor, 1:20000) secondary antibody was used to image primary antibody detection with the Odyssey V3 imaging system. Total protein content was measured by Ponceau S staining (Figure S7). Intensities of protein detection were quantified using Image Studio. DNA content rather than protein content was used as the loading control because β-less mice have a different reference protein composition (tubulin, actin, etc.) likely due to the aberrant white-like morphology.

### 2.10. Morphometric, immunohistochemistry and Transmission Electron Microscopy

Paraffin embedded sections were stained with hematoxylin and eosin and immunostained for uncoupling protein 1 (UCP1), tyrosine hydroxylase (TH) and vesicular nucleotide transporter (VNUT). For the TEM analysis, epon-Araldite embedded sections were stained with lead citrate and examined with a CM10 transmission electron microscope. Full details are provided in [SI Materials and Methods](#).

### 2.11. Adipogenesis induction and experimental treatments

Immortalized iBAT pre adipocytes from wt and  $\beta$ -less mice were differentiated with minimal adipogenic medium (MAM) with or without NE, ATP $\gamma$ S or isoproterenol. Full details are provided in [SI Materials and Methods](#).

### 2.12. Statistical analysis

Unless stated otherwise data were analyzed with Student's t-test or ANOVA followed by Tukey HSD post hoc test using STATISTICA (StatSoft Inc.).

## 3. RESULTS

### 3.1. Individual vulnerability to stress-induced obesity is determined by the pre-stress level of adaptive thermogenesis

We used the  $\beta$ -less mouse model [19] as a sensitizer tool to identify and test  $\beta$ -AR independent mechanisms of BAT activation. Chronic cold exposure is a potent stimulus for recruitment and activation of the

BAT [9,41–43]. We tested the effect of acclimatizing  $\beta$ -less mice to mild cold (14 °C) on metabolic adaptation and BAT recruitment (exposure to 4 °C was avoided based on the severe cold intolerance of this strain [19]). Unexpectedly,  $\beta$ -less mice acclimatized well to mild cold, showing increased BAT UCP1 expression and improved metabolic functions (Figure 1A–D). To further explore the capacity of this alternative mechanism, we tested the behavioral response of  $\beta$ -less and wt mice to a range of temperatures at or above the room temperature of 22 °C using the thermal gradient test (Figure S1A,B). As expected, wt mice showed a marked preference for temperatures above 29 °C, which is within the expected thermoneutral zone of the species [26,27]. Conversely,  $\beta$ -less mice did not manifest a significant preference for zones above 29 °C or below 23 °C (Figure S1B), suggesting altered thermal preference of  $\beta$ -less compared to wt mice. Using 7T-MRI, we documented the absence of detectable BAT and increased subcutaneous fat deposition in the cervical region corresponding to the interscapular BAT (but not in a more caudal cross sections) of  $\beta$ -less compared to wt mice acclimatized to room temperature (Figure S1C), suggesting that altered insulation in  $\beta$ -less mice could contribute to the impaired thermogenic profile [44].

The observed restoration of UCP1 and thermogenesis induced by mild cold acclimatization in  $\beta$ -less mice advocates for the existence of alternative  $\beta$ AR-independent mechanisms of BAT activation. This finding prompted us to determine whether the same result could be replicated in a model relevant for obesity and type 2 diabetes [28]. Acute social defeat elicits a  $\beta$ -AR dependent iBAT thermogenesis (Figure S2) [45] by activating a neural pathway largely overlapping with

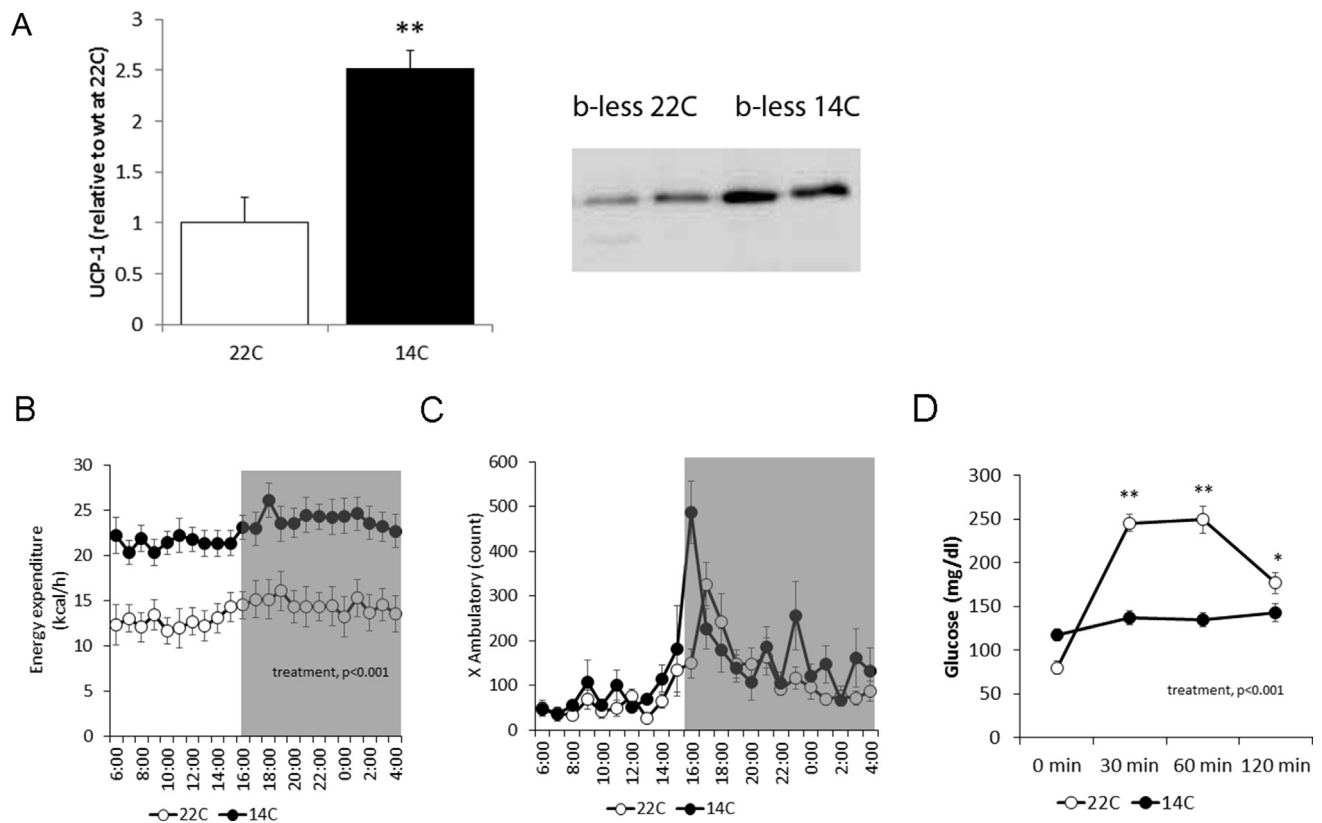


**Figure 1: Mild cold (14 °C)-induced browning and improved metabolic functions in  $\beta$ -less mice. A)** BAT UCP1 quantification and representative gel showing UCP1 band and total protein. **B)** Energy expenditure assessed via indirect calorimetry. Heat is expressed as Kcal/h and analyzed with body weight as continuous predictor in an ANCOVA model [34] ( $F(1,10) = 10.4$ ,  $p < 0.001$ ). **C)** Locomotor activity in the indirect calorimetry chambers. **D)** Glucose tolerance test (Treatment  $\times$  time  $F(3,33) = 37.5$ ,  $p < 0.00001$ ). \* $p < 0.05$ , \*\* $p < 0.01$ .  $N = 6-7$ .

the one induced by cold exposure [45]. We thus exposed wt and  $\beta$ -less mice to a model of chronic subordination stress-induced obesity and type 2 diabetes [28]. We hypothesized that chronic subordination stress would over time activate the BAT, and possibly mediate resilience to obesity in  $\beta$ -less mice, on the basis of the observed  $\beta$ AR-independent thermogenic potential. As expected [28,31,32], subordinate wt mice developed sustained hyperphagia and were vulnerable to diet-induced obesity and hyperglycemia in presence of minimal

changes in energy expenditure, which were observed only in the light phase (Figures 2 and S3). Conversely, subordinate  $\beta$ -less mice showed lower weight and fat mass gain, normalized energy expenditure and fasting glycemia, and improved glucose tolerance compared to controls in spite of being hyperphagic (Figures 2 and S3). It is worth emphasizing that although  $\beta$ -less mice showed less immobility in the FST and higher plasma corticosterone compared to wt, social subordination exerted similar depressive-like effects in both wt and  $\beta$ -less

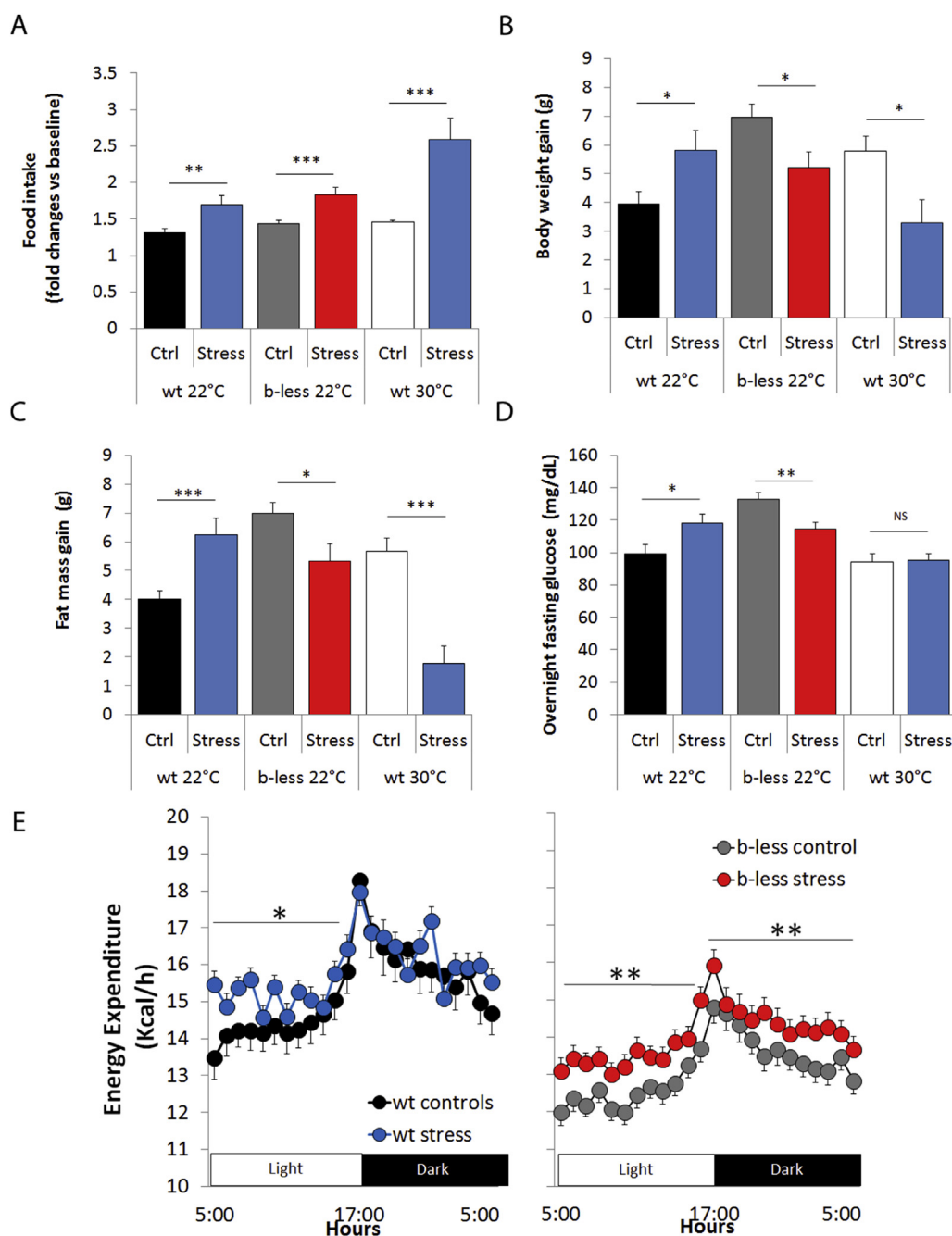


**Figure 2:**  $\beta$ -less housed at 22 °C and wt-mice housed at 30 °C are resistant to chronic subordination stress-induced obesity. **A)** Food intake was measured daily and expressed as average Kcal/day normalized over baseline pre-stress values (wt 22 °C,  $t_{30} = 3.2$ ,  $p < 0.01$ ;  $\beta$ -less,  $t_{49} = 3.6$ ,  $p < 0.001$ ; wt 30 °C,  $t_{18} = 4.6$ ,  $p < 0.001$ ). **B)** Body weight gain (wt 22 °C,  $t_{34} = 2.4$ ,  $p < 0.05$ ;  $\beta$ -less,  $t_{54} = 2.4$ ,  $p < 0.05$ ; wt 30 °C,  $t_{18} = 2.7$ ,  $p < 0.05$ ). **C)** Fat mass gain (wt 22 °C,  $t_{34} = 3.7$ ,  $p < 0.001$ ;  $\beta$ -less,  $t_{54} = 2.4$ ,  $p < 0.05$ ; wt 30 °C,  $t_{18} = 5.4$ ,  $p < 0.001$ ). **D)** Overnight fasting glucose (wt 22 °C,  $t_{25} = 2.3$ ,  $p < 0.05$ ;  $\beta$ -less,  $t_{50} = 2.9$ ,  $p < 0.01$ ). **E)** Energy expenditure ( $F_{(11,759)} = 1.7$ ,  $p = 0.05$ ).  $N = 11-29$ . \* $p < 0.05$ , \*\* $p < 0.01$ , \*\*\* $p < 0.001$ .

mice at neuroendocrine as well as behavioral levels (Figure 3 and Table S1). The only exception to this was the FST in which  $\beta$ -less, but not wt, mice manifested exacerbated stress-induced immobility (Figure 3C). Overall, these behavioral results rule out the possibility that  $\beta$ -less are resistant to obesity when exposed to CSS because of an overall stress-resilient phenotype.

Based on the altered thermoneutrality set point manifested by  $\beta$ -less mice (see above), we next asked whether their stress-induced obesity resistant phenotype could be recapitulated in wt mice by lowering their basal BAT function and adaptive thermogenesis by acclimatization to thermoneutrality (30 °C). Consistent with this hypothesis, wt mice housed at 30 °C were resilient to stress-induced obesity and remained normoglycemic despite hyperphagia (Figures 2, S3), overall mirroring the phenotype of subordinate  $\beta$ -less mice and in sharp contrast to subordinate wt mice at 22 °C. In conclusion, we showed that the resilience to stress-induced obesity is determined by low pre-stress level of adaptive thermogenesis.

### 3.2. Stress-induced browning of the BAT

We next asked whether resilience to stress-induced obesity was mediated by BAT activation/recruitment. As expected [19], the BAT of

$\beta$ -less control mice at 22 °C and wt mice housed at 30 °C was characterized by prevailing “white-like” unilocular UCP1-negative adipocytes (Figure 4A). A low amount of scattered multilocular UCP1-positive adipocytes (~30% in  $\beta$ -less at 22 °C and ~45% in wt at 30 °C) were still present in parallel with low UCP1 protein detected by western blot (Figure 4A). Ultrastructural analysis of the BAT of  $\beta$ -less mice revealed that the unilocular adipocytes had predominantly roundish shaped mitochondria similar to those found in “classical” brown adipocytes [41,42] although smaller in size and at a lower density (Figure 5A, B). Remarkably, the BAT obtained from subordinate  $\beta$ -less mice was largely normalized (Figure 4A), and the BAT of subordinate wt mice at 30 °C was fully normalized in spite of mice being housed at thermoneutrality (Figure 4A). UCP1-immunohistochemistry was well conserved recapitulating bona fide brown adipose tissue [46,47] rich in multilocular UCP1-positive adipocytes (~70% and ~100% of the adipocytes in  $\beta$ -less and wt at 30 °C respectively) (Figure 4A). UCP1 protein was increased in the BAT of subordinate  $\beta$ -less at 22 °C and wt mice at 30 °C, this induction being larger in magnitude in wt mice (Figure 4A, B).

Gene-expression profiling of the BAT of  $\beta$ -less mice demonstrated the downregulation of brown fat cell differentiation, electron transport

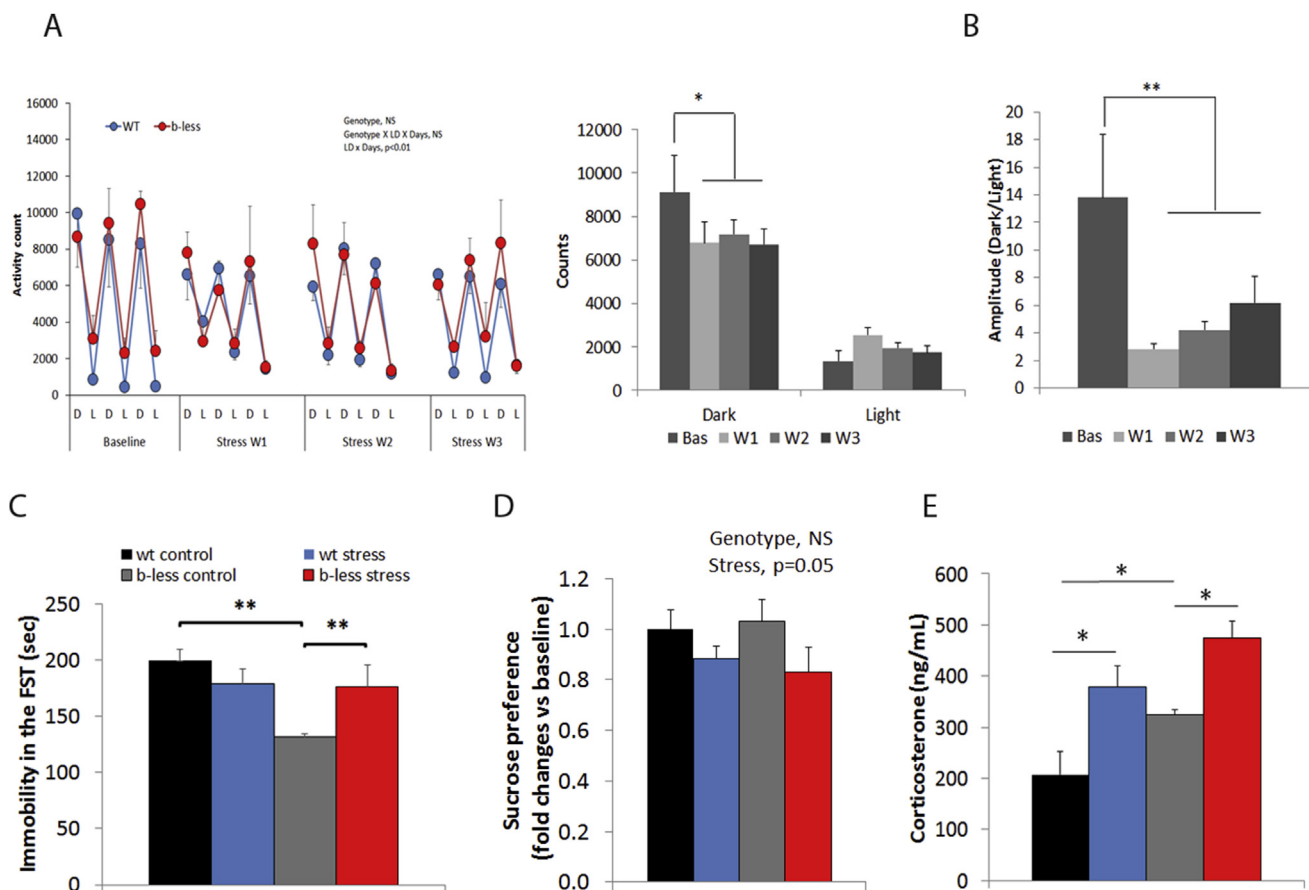


**Figure 3: Chronic Subordination Stress-induced depression-like behavior in wt and  $\beta$ -less mice.** **A)** Wt and  $\beta$ -less mice showed a similar depression of home-cage activity in the dark (active) phase. Data were analyzed with a 3-way ANOVA with Light/Dark phase and Weeks as within factors and genotype as between factor. Statistical analysis showed no effect for the genotype ( $F(1,9) = 0.4$ , ns) and a significant interaction between Light/Dark and weeks ( $F(3,27) = 3.96$ ,  $p < 0.05$ ). Post hoc analysis showed a significant decrease in activity for weeks 1 and 3 compared to baseline,  $p < 0.05$ . Graph show the raw activity data D = Dark, L = Light, W = week). **B)** Similar to total activity, the amplitude of the circadian activity pattern (Dark/Light), was affected by CSS independently from the genotype (weeks  $F(3,27) = 4.1$ ,  $p < 0.05$ ) (Bas = Baseline, W = week of stress). **C)** Forced swim test ( $F(1,19) = 6.1$ ,  $p < 0.05$ ). **D)** Sucrose preference test (treatment,  $F(1,18) = 4.3$ ,  $p = 0.051$ ). **E)** Plasma Corticosterone in response to a heterotypical stress, i.e. forced swim test, (genotype,  $F(1,18) = 7.4$ ,  $p < 0.05$ ; treatment,  $F(1,18) = 16.9$ ,  $p < 0.00001$ ).  $N = 5-7$ . \* $p < 0.05$ , \*\* $p < 0.01$ .

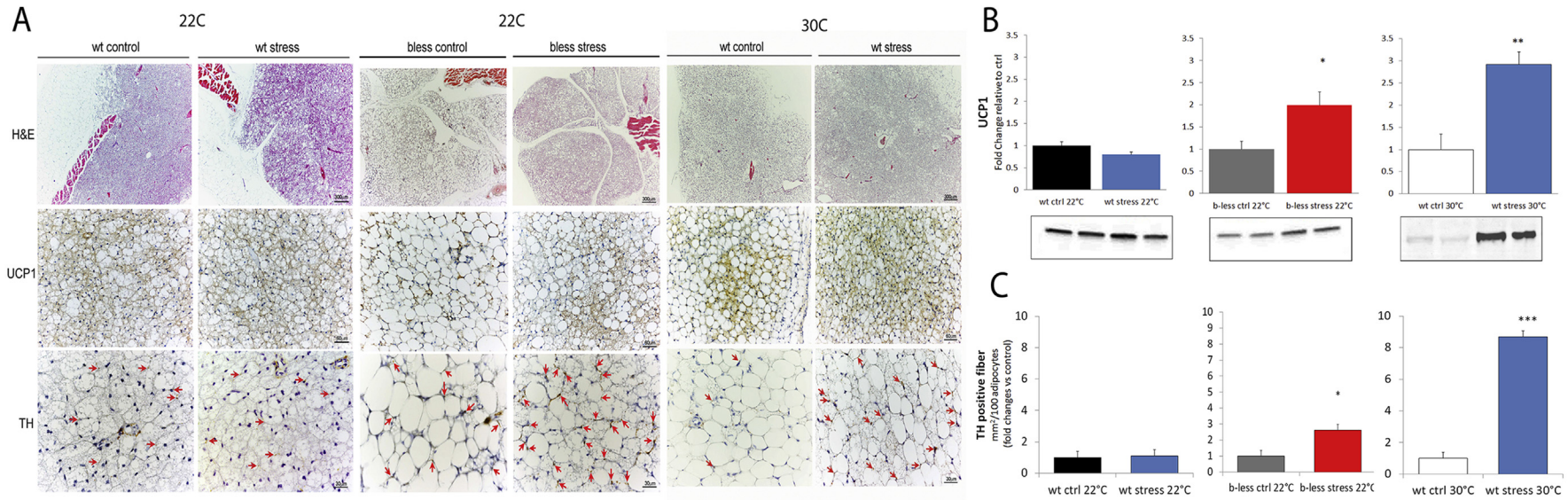


**Figure 4: Chronic subordination stress normalizes iBAT morphology, UCP1 and sympathetic innervation in  $\beta$ -less housed at 22 °C and wt-mice housed at 30 °C. A)** Immuno-morphological analysis of the iBAT in control and stress wt and  $\beta$ -less mice. Upper panels, hematoxylin and eosin (H&E); Central panels, uncoupling protein 1 (UCP1) immunohistochemistry (IHC); Lower panels, tyrosine hydroxylase (TH) IHC. Red arrows highlight nerve terminals. **B)** UCP1 western blot in the iBAT ( $\beta$ -less,  $t_{12} = 2.8$ ,  $p < 0.05$ ; wt 30 °C,  $t_6 = 4.3$ ,  $p < 0.01$ ). **C)** TH fiber density in the iBAT ( $\beta$ -less,  $t_{10} = 2.3$ ,  $p < 0.05$ ; wt 30 °C,  $t_{10} = 11.4$ ,  $p < 0.0001$ ). N = 6–8.

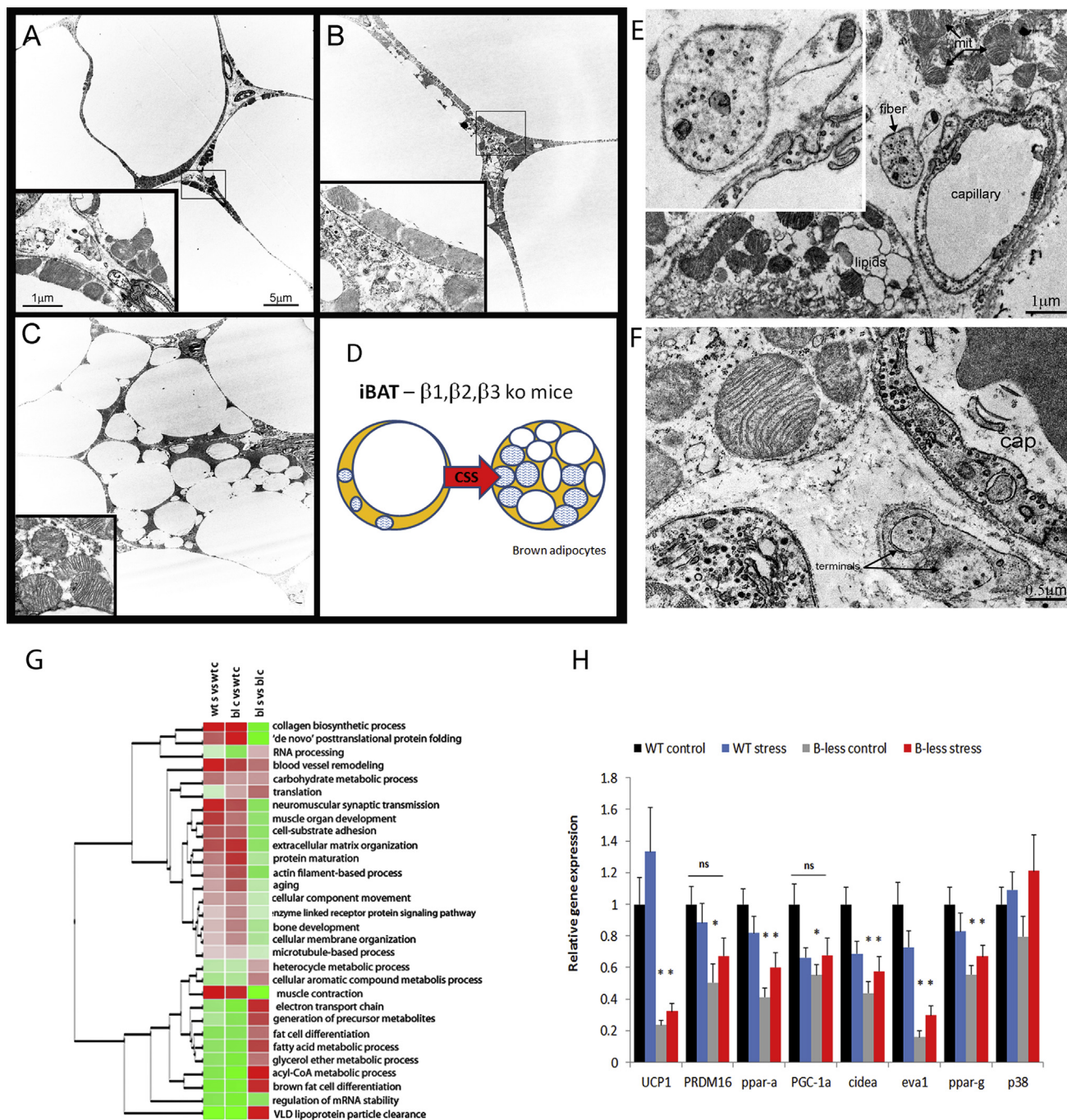


**Figure 5: Transmission Electron Microscopy and molecular analyses.** **A)** A representative unilocular adipocyte in  $\beta$ -less control mice. **B)** A representative unilocular adipocytes in chronic subordination stress (CSS)-exposed  $\beta$ -less mice. **C)** A representative paucilocular adipocyte in CSS  $\beta$ -less mice. Inserts show a magnification of mitochondria. **D)** Cartoon of the morphological changes induced by CSS. **E,F)** Representative nerve terminals in CSS  $\beta$ -less mice. **G)** The heat map describes the odds-ratio for 30 shared GO terms among all experimental groups created with Gtools (<http://www.gtools.org/>). Average odd-ratios for each GO term were used to cluster GO terms based on similar pathway direction in expression. Further details are provided as [Supplementary Material](#). **H)** Quantitative real time PCR of classical brown adipocyte molecular markers. Data are expressed as fold changes vs wt controls. N = 11–13.

chain and, several lipid metabolism pathways compared to wild type (Figure 5G; Table S2). Conversely, molecular pathways associated with the myogenic lineage were upregulated in the BAT of  $\beta$ -less mice compared to wild type supporting a switch from brown to “muscle-like” programming in absence of  $\beta$ AR signaling [48,49]

(Figure 5G; Table S2). Subordination stress induced a global gene reprogramming in the BAT of  $\beta$ -less mice consisting in the down-regulation of myogenic/skeletal muscle pathways and the upregulation of mitochondria/lipid metabolism/brown cell differentiation pathways (Figure 5C). The gene expression of most brown adipocyte



markers (e.g. PRDM16, PGC1 $\alpha$  and Eva1, but not UCP1), down-regulated in  $\beta$ -less compared to controls, was partially normalized by stress (Figure 5H). It must be noted that UCP1 mRNA is only rapidly and transiently induced by acute cold stimulation while its level is not substantially altered following cold acclimation [50]. Having demonstrated a stress-induced recruitment of brown adipocytes and increased UCP1 protein levels (Figure 4A, B), it is thus likely that changes in UCP1 mRNA expression occurred earlier in the social defeat protocol and were not detectable when mice were sacrificed. Finally, we asked the question if the stress-induced browning was generalized throughout the adipose organ or specific to the classical interscapular BAT. Molecular markers of beige adipocytes (such as UCP1, PGC1 $\alpha$ , TMEM26, HOX9) were upregulated in the subcutaneous white adipose tissue (scWAT) of subordinate  $\beta$ -less mice (Figure S4A), but we could not detect multilocular UCP1 expressing adipocytes or UCP1 protein by western blot in the same fat pad (Figure S4B,C). This evidence convincingly demonstrates that subordination stress elicits a selective browning of the interscapular BAT and provide additional support to the observation that beige adipocyte programming in the scWAT is at least in part  $\beta$ ARs-independent [51].

### 3.3. Identification of a sympathetic/brown adipocyte purinergic pathway

The selective stress-induced browning of the BAT suggested that a local autocrine/paracrine rather than an endocrine circulating factor was the most likely mechanistic candidate. In support, subordination stress induced a significant increase in tyrosine hydroxylase (TH)-positive sympathetic fibers density in the BAT (and not scWAT) of  $\beta$ -less mice and wt mice housed at 30 °C but not of wt housed at 22 °C (Figure 4A, C). This result prompted us to test the role of norepinephrine and  $\alpha$ ARs in the stress-induced browning of the BAT observed in  $\beta$ -less mice. The  $\alpha$ 1<sub>A</sub>-AR,  $\alpha$ 1<sub>D</sub>-AR and  $\alpha$ 2<sub>A</sub>-AR [52] were all downregulated in the BAT of  $\beta$ -less control mice compared to wt (Figure S5A) and could not be fully rescued by subordination stress (Figure S5A). Additionally, subordinate  $\beta$ -less mice did not show the normal novelty-induced and norepinephrine-mediated [9,42] increase in VO<sub>2</sub>, which was conserved in wt mice (Figure S5C). Finally, norepinephrine increased UCP1 mRNA in wt but not  $\beta$ -less brown adipocytes in vitro (Figure S5B).

Overall, stress increased sympathetic innervation of the iBAT without a testable contribution of adrenergic signaling to browning in mice deficient of the  $\beta$ ARs. This finding led us to investigate nerve-secreted factors other than norepinephrine for this role. TEM examination of the nerve terminals in the BAT of  $\beta$ -less mice revealed a normal morphology, with fibers containing small vesicles and limited dense-core vesicles (Figure 5E, F). The sympathetic nerve secretome is incompletely understood [53–56], and recent evidences suggest that the purinergic system might play a functional role in the BAT [57,58]. Here we showed that both sympathetic nerve fibers innervating the BAT and brown adipocytes express the VNUT (vesicular nucleotide transporter [59]), which is required for ATP storage in secretory vesicles [60] (Figure 6A, S6A,B). Remarkably, we also identified VNUT positive nerve fibers and brown adipocytes in human BAT (Figure 7). In both mice and humans VNUT expression was restricted to brown adipocytes and not expressed by white or “white-like adipocytes” (Figures 6A, 7 and S6A,B). VNUT mRNA was downregulated in the BAT of both  $\beta$ -less and wt mice acclimatized to thermoneutrality (Figure 6B). The same experimental groups also showed a down-regulation of most of the P1 and P2 receptor subtypes expressed by brown adipocytes [57,58,61] (Figure 6B), overall demonstrating that the purinergic signaling is downregulated in conditions promoting low

adaptive thermogenesis. VNUT protein and mRNA expression were largely normalized in subordinate  $\beta$ -less mice (Figures 6A, S6C). Similarly, stress in  $\beta$ -less mice led to a significant upregulation of P2RX5, a recently identified brown adipocyte membrane marker [57] (Figure S6C). Similar changes, although of lower magnitude, were observed in subordinate wt mice housed at 30 °C without any detectable change in wt mice acclimatized to 22 °C (Figure S6C). Overall, our results suggest that the purinergic tone to the interscapular BAT is plastic, as it appears to be downregulated in conditions promoting low adaptive thermogenesis and inducible by stress. Because of the lack of selective P2RX5 agonists, we tested the contribution of P2RXs incubating brown adipocytes in vitro with ATP $\gamma$ S, a hydrolysis-resistant P2 agonist. ATP $\gamma$ S enhanced UCP1 expression in both wt and  $\beta$ -less brown adipocytes (Figure 6C), supporting the conclusion that ATP might mediate browning of the BAT in condition of low adaptive thermogenesis and  $\beta$ AR deficiency.

## 4. DISCUSSION

Chronic stress is a major risk factor for both psychiatric and metabolic disorders. Significant progress has been made on the molecular mechanisms of resilience to stress-induced psychiatric disorders such as major depression and anxiety [e.g. 62,63]. Conversely, a functional explanation for the bidirectional effect of stress on energy balance, observed in humans and animal models, is still missing [4,29,64–69]. Here we demonstrated that the level of adaptive thermogenesis and the functional status of brown adipose tissue determine the resilience or the vulnerability to stress-induced obesity in mice in spite of similar level of hyperphagia, offering a key to interpret the dichotomous effect of stress on energy balance. We also demonstrated that  $\beta$ ARs are dispensable for cold- and subordination stress-induced BAT browning, and, finally, our data suggest the existence of an inducible sympathetic/brown adipocyte purinergic pathway of browning in mice and showed that it is conserved in humans, therefore presenting a new potential therapeutic target to address stress related metabolic disorders.

### 4.1. Stress, adaptive thermogenesis and obesity

To model the impact of psychosocial stress on metabolism, we used a validated model of human stress-induced disease that mimics the role of socio-economic status on health [70–72]. Remarkably, different models of chronic psychosocial stress resulting in a similar hypothalamus-pituitary adrenocortical (HPA)-axis activation and depression-like behavior [62,73] induce opposite effects on energy balance [28,31,74, reviewed in 68,69]. For example, in the chronic social defeat stress model (CSDS), subordinate mice consistently manifest weight and fat mass loss during the defeat phase [74]. Conversely, in our model, subordinate mice manifest weight gain and vulnerability to obesity [28,31,32]. Here we showed that the metabolic consequence of chronic subordination stress is dependent upon the basal level of adaptive thermogenesis and BAT functions. Specifically, in conditions promoting low BAT differentiation/activity, such as acclimation to thermoneutrality or genetic predisposition ( $\beta$ -less mice), subordination stress acted as a stimulus for browning and thermogenesis, thereby exerting a negative effect on energy balance. Conversely, when BAT activity was tonically stimulated, e.g. mice housed at room temperature, subordination stress only marginally affected energy expenditure and BAT function and this was not sufficient to compensate the stress-induced hyperphagia thus resulting in obesity and type 2 diabetes-like conditions [28,32,72]. Interestingly, the metabolic (but not the behavioral) phenotype of the subordinate mice in the CSDS [e.g. 74] resembles that of the dominant animal in

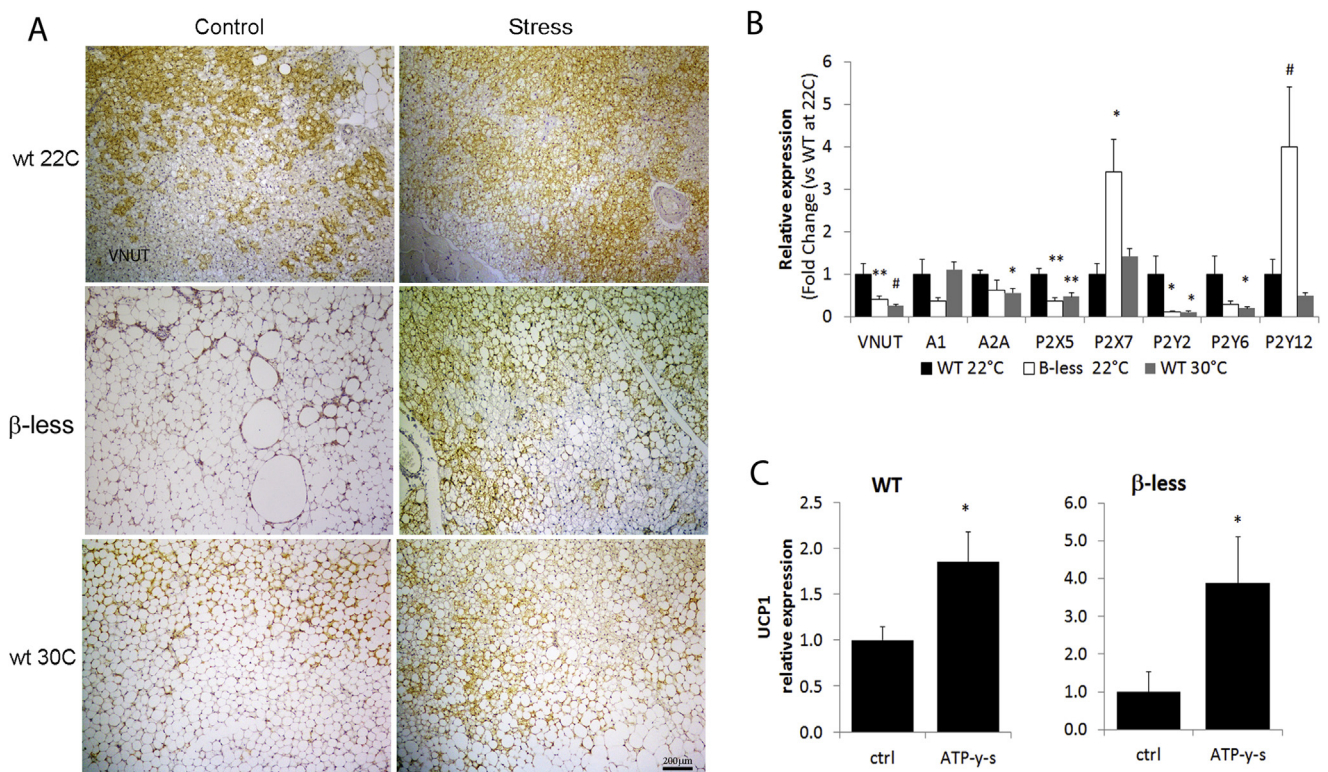


**Figure 6: Immuno-morphological and molecular evidence of purinergic modulation of browning in mice.** **A)** Immunohistochemical evidence of VNUT expression in mice BAT. VNUT was downregulated in  $\beta$ -less and wt housed at 30 °C, and normalized by subordination stress. **B)** Downregulation of purinergic signaling in the iBAT of  $\beta$ -less and wt mice at thermoneutrality. N = 8–10. **C)** ATP $\gamma$ S increase UCP1 mRNA in wt and  $\beta$ -less brown adipocytes in vitro. N = 4–6.

our stress model. Dominant mice are in fact resistant to diet induced obesity despite being hyperphagic and in presence of increased energy expenditure and sympathetic innervation to fat pads [28,31]. Overall, our result suggests that regarding stress-induced obesity, resilience occurs in conditions leading to sympathetic activation of the BAT and enhanced thermogenesis, while vulnerability occurs when stress-induced hyperphagia is not compensated by enhanced thermogenesis. An increase in BAT function has consistently been associated with decreased body weight and adiposity as well as improved lipid and glucose homeostasis [9,75]. However, the classical animal models of adipose organ browning, i.e. chronic 4 °C exposure, cancer cachexia and  $\beta$ AR agonist treatment [9,17,76] bear very limited translational relevance. Our naturalistic model of social stress-inducible BAT browning at thermoneutrality is of main translational relevance because humans live mostly at thermal comfort levels which induce low sympathetic tone and  $\beta$ AR expression. This parallel makes our mechanistic findings (discussed below) relevant to inform on novel therapeutic approaches for obesity and diabetes via the stimulation of BAT function.

#### 4.2. $\beta$ -Adrenergic receptors are dispensable for browning

We provided direct evidence that  $\beta$ ARs are dispensable for the gene program, morphology and, function of the brown adipose tissue. We also identified a previously unrecognized, altered thermogenic phenotype in the absence of  $\beta$ ARs, which accounts for the discrepancy. Indeed,  $\beta$ -less mice manifest an altered thermoneutrality set-point as demonstrated by the lack of behavioral preference for temperatures comprised between 29 °C and 33 °C, which is within the normal thermoneutrality range for mice. Additionally, we also

demonstrated that the BAT of  $\beta$ -less mice can undergo browning in conditions of mild cold exposure, thus showing a normal plasticity and adaptation to thermogenic demands. The 7T-MRI data suggest that an atypical thermal insulation could explain the altered, critical lower temperature set point, although temperature perception and/or neural regulation of BAT activity could also play a role [42,44].

Notably, stress-elicited browning was limited to the classical brown depot, BAT, and was not generalized to scWAT, overall setting subordination stress apart from other browning-eliciting stimuli such as cold or cancer that are linked to a generalized browning of the adipose organ. Accordingly, our findings have important implications for brown adipocyte biology. BAT from  $\beta$ ARs deficient, denervated or, catecholamine-deficient mice, contains large cells with unilocular triglyceride deposits and limited UCP1 [19,77,78], showing features of both brown and white adipocytes [47]. These results indicated that  $\beta$ ARs are necessary for normal BAT morphology but also that  $\beta$ ARs are somehow redundant in BAT-mediated UCP1 expression [19]. Here we demonstrated that  $\beta$ -less brown adipocytes have prevalent, small size brown-like mitochondria and that the BAT manifests a global gene reprogramming characterized by high expression of skeletal muscle markers and low expression of classical brown adipocyte, mitochondria and lipid metabolism pathways/markers, which is consistent with their origin from the myogenic lineage [48,49]. Critically, stress led to a prevailing population of multilocular UCP1-expressing adipocytes with increased density of classical brown mitochondria, partially normalized gene programming typical of brown adipocytes and global normalization of the transcriptome. Therefore, we conclude that the “white-like adipocytes” detectable in the BAT of the  $\beta$ -less mice as well as in wt mice housed at thermoneutrality should be considered “de-

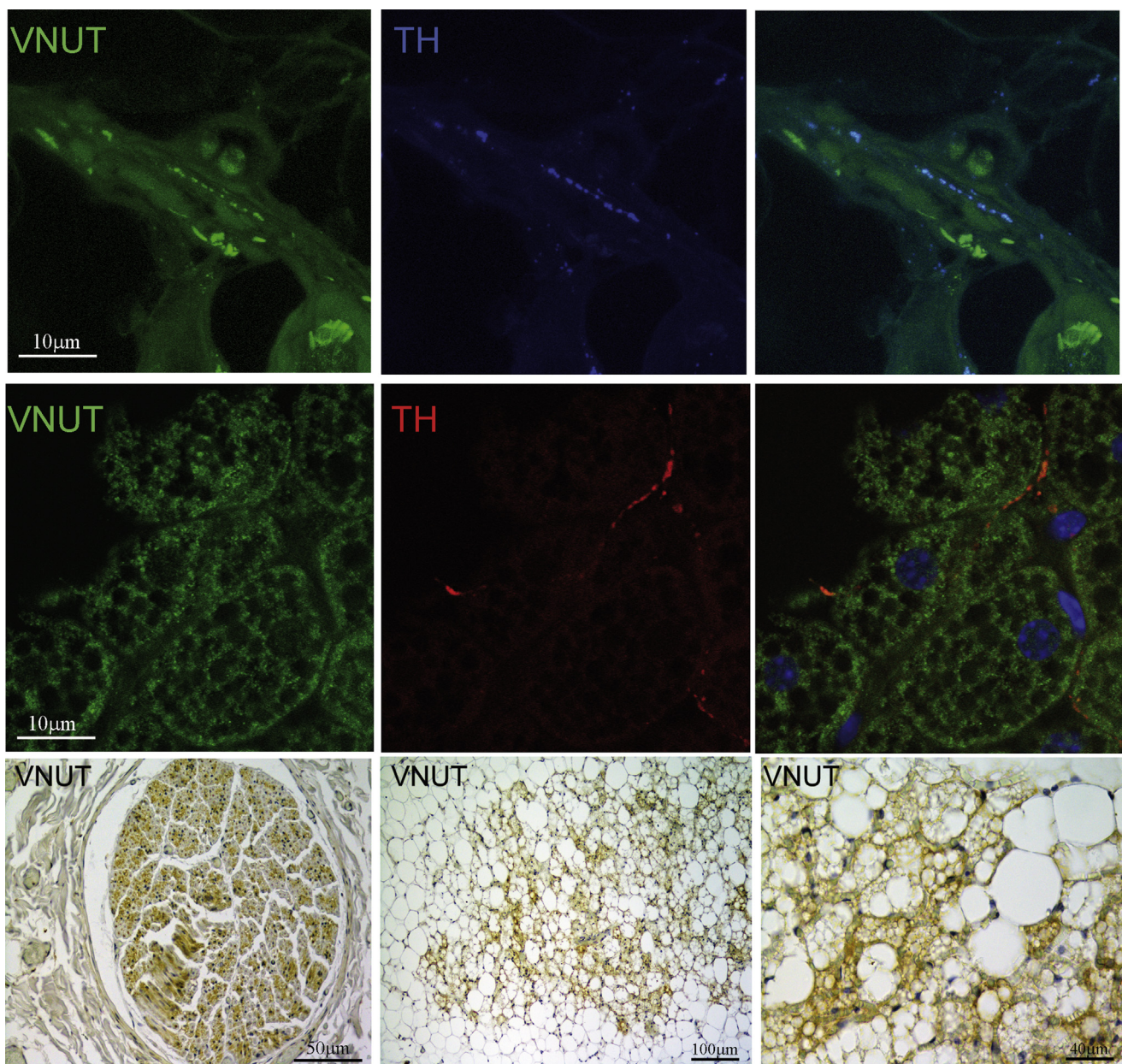


**Figure 7: Immuno-morphological evidence of VNUT expression in human perithyroid BAT.** Representative interlobar nerves (upper panels and lower left panel) and BAT parenchyma (middle panels and lower middle and right panels).

differentiated” or quiescent brown adipocytes that, in presence of appropriate stimuli, are activated to acquire a normal morphology and function. An alternative, although less likely, hypothesis is stress-induced tissue remodeling by de novo adipogenesis [79,80].

#### 4.3. Identification of an inducible sympathetic/brown adipocyte purinergic pathway

One of the main findings of this study is that stress led to a basal adaptive thermogenesis-dependent increase in sympathetic innervation and function of the BAT. Cold and acute social defeat have been shown to activate the sympathetic innervation to the BAT [42,44]. After having demonstrated that  $\beta$ AR are dispensable for browning and that  $\alpha$ AR activation does not increase UCP1 expression in  $\beta$ -less mice, we

identified a sympathetic/brown adipocyte purinergic pathway in the BAT which has the following characteristics: i) it is down-regulated in conditions of low adaptive thermogenesis requirement; ii) it mediates browning in wt and  $\beta$ -less brown adipocytes; iii) it is conserved in human BAT.

Purinergic/noradrenergic co-transmission has been previously demonstrated in the central nervous system and peripheral organs [54,81]. In purinergic cells, the nucleotides transporter VNUT is responsible for ATP storage in secretory vesicles [54,59,60]. The accumulated ATP is exocytosed upon stimulation and binds to purinergic receptors expressed by postsynaptic target cells. ATP can also be converted to adenosine via ectonucleotidase [54,58,60]. Increased ATP/adenosine secretion induced by electric field potential has been

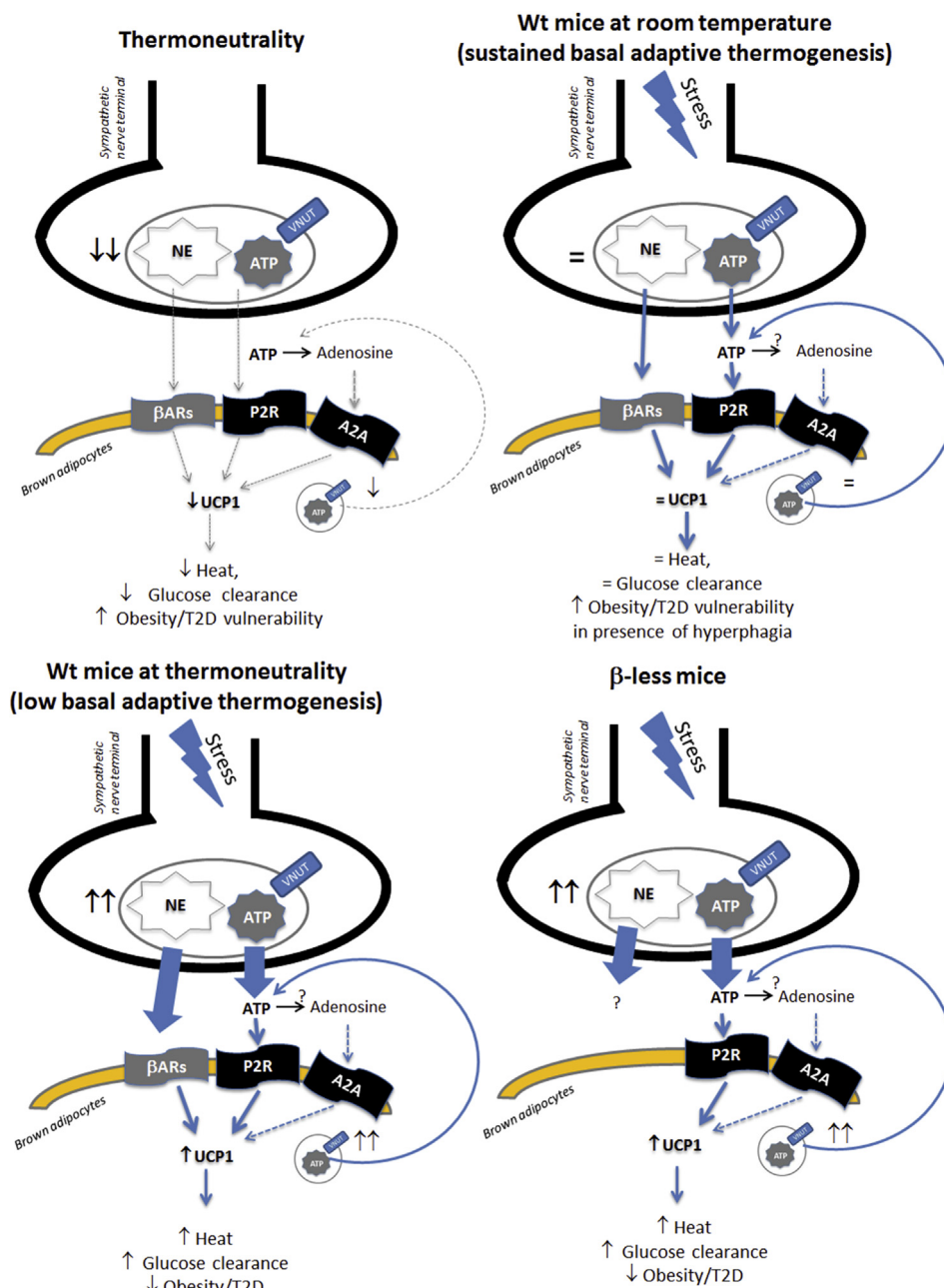


**Figure 8: Proposed model of stress-induced sympathetic adrenergic and purinergic modulation of BAT.** Proposed mechanistic model of synergistic modulation of brown adipocyte functions by sympathetic adrenergic and purinergic pathways. See text for details. ATP conversion to adenosine and A2A modulation of browning has been demonstrated for cold-induced browning by Gnad et al., 2014 [58].

recently demonstrated in BAT but the source of ATP was not identified [58]. Similarly, several purinergic receptors are expressed by brown adipocytes [55,58], but their functional role remains so far poorly characterized. Recent work established a role for adenosine/A2A receptor in cold-associated browning [58] and a selective expression of the P2RX5 in brown adipocytes [57]. Here we demonstrated that VNUT is expressed in sympathetic nerves innervating the brown adipose tissue as well as in brown adipocytes (but not in white or “de-differentiated” brown adipocytes) suggesting a double source for intra BAT ATP secretion. Of primary importance, we demonstrated that the same pattern of expression is also conserved in human BAT. It must be noted that in mice, VNUT, P2RX5 and several other P1R, P2RX and P2RY

receptors were downregulated in conditions of thermoneutrality and  $\beta$ AR deficiency, and P2RX5 was upregulated by stress, overall indicating a critical role for nerve released ATP in triggering BAT activation and differentiation under low adaptive thermogenesis. We also demonstrated that ATP induced browning in vitro is independent of  $\beta$ ARs expression. Because of the complexity and redundancy of the purinergic receptor system it is likely that more than one receptor, including A2A [58] and P2RX5 [57], modulates brown adipocyte differentiation and thermogenic functions. At the same time, the complexity of the purinergic receptor system could be considered a keystone accounting for the paradoxical viability of mice genetically deficient for all known  $\beta$ ARs.

## 5. CONCLUSION

In conclusion, our study and others [57,58,61] support a model in which adrenergic and purinergic sympathetic pathways exert redundant functions and are synergistic in modulating brown adipose tissue functions (Figure 8). Further experiments are required to clarify the mechanistic validity of the proposed model including the use of genetically engineered mouse models of impaired ATP secretion [e.g. 82]. Based on the large body of evidence supporting a main functional role for adrenergic transmission in the BAT [9], we propose that the adrenergic pathway prevails in regulating brown adipocyte differentiation and function in conditions of sustained thermogenesis via activation of  $\beta$ ARs. However, in conditions of low adaptive thermogenesis (e.g. thermoneutrality), both the purinergic and the adrenergic pathways can be activated to modulate brown adipocyte functions. The latter conclusion suggests that the purinergic system could offer a new viable candidate to target brown adipocytes so to develop anti-obesity and anti-diabetic therapies devoid of the cardiovascular side effects associated with the use of  $\beta$ ARs agonists.

## ACKNOWLEDGMENTS

Supported by NIH/NIDDK DK102496, NIH/NIA AG043972, University of Minnesota Medical School and University of Minnesota Foundation to A.B., DIABAT-FP7HEALTH-F2-2011-278373 (SC), BIO2011-27069, Spanish Ministry of Economy and Competitiveness (JD), EU FP7-PEOPLE 316861 (C.Cabuk), Doctoral Dissertation Fellowship, University of Minnesota (C.Cero). TVP is supported by MRC, Wellcome Trust, BetaBat, and BBSRC. We wish to thank B. B. Lowell for providing the  $\beta$ -less mice and feedback on our study, W. Engeland for the corticosterone assay, J. McCallum, C. Erickson and J. Asturias for technical help, and M. Wessendorf for the TGT test.

## CONFLICT OF INTEREST

None declared.

## APPENDIX A. SUPPLEMENTARY MATERIAL

Supplementary material related to this article can be found at <http://dx.doi.org/10.1016/j.molmet.2015.10.005>.

## REFERENCES

- [1] McEroy, S.L., Kotwal, R., Malhotra, S., Nelson, E.B., Keck, P.E., Nemeroff, C.B., 2004. Are mood disorders and obesity related? A review for the mental health professional. *Journal of Clinical Psychiatry* 65:634–651.
- [2] National Task Force on the Prevention and Treatment of Obesity, 2000. Overweight, obesity, and health risk. *Archives of Internal Medicine* 160:898–904.
- [3] Kiecolt-Glaser, J.K., Habash, D.L., Fagundes, C.P., Andridge, R., Peng, J., Malarkey, W.B., et al., 2015. Daily stressors, past depression, and metabolic responses to high-fat meals: a novel path to obesity. *Biological Psychiatry* 77: 653–660.
- [4] Dallman, M.F., 2010. Stress-induced obesity and the emotional nervous system. *Trends in Endocrinology and Metabolism* 21:159–165.
- [5] Schwartz, M.W., Woods, S.C., Porte Jr., D., Seeley, R.J., Baskin, D.G., 2000. Central nervous system control of food intake. *Nature* 404:661–671.
- [6] Lowell, B.B., Spiegelman, B.M., 2000. Towards a molecular understanding of adaptive thermogenesis. *Nature* 404:652–660.
- [7] Rodgers, R.J., Tschöp, M.H., Wilding, J.P., 2012. Anti-obesity drugs: past, present and future. *Disease Models & Mechanisms* 5:621–626.
- [8] Tseng, Y.H., Cypess, A.M., Kahn, C.R., 2010. Cellular bioenergetics as a target for obesity therapy. *Nature Reviews Drug Discovery* 9:465–482.
- [9] Cannon, B., Nedergaard, J., 2004. Brown adipose tissue: function and physiological significance. *Physiological Reviews* 84:277–359.
- [10] Peirce, V., Vidal-Puig, A., 2013. Regulation of glucose homeostasis by brown adipose tissue. *Lancet Diabetes & Endocrinology* 1:353–360.
- [11] Cypess, A.M., Lehman, S., Williams, G., Tal, I., Rodman, D., et al., 2009. Identification and importance of brown adipose tissue in adult humans. *New England Journal of Medicine* 360:1509–1517.
- [12] Virtanen, K.A., Lidell, M.E., Orava, J., Heglind, M., Westergren, R., et al., 2009. Functional brown adipose tissue in healthy adults. *New England Journal of Medicine* 360:1518–1525.
- [13] van Marken Lichtenbelt, W.D., Vanhommerig, J.W., Smulders, N.M., Drossaerts, J.M., Kemerink, G.J., et al., 2009. Cold-activated brown adipose tissue in healthy men. *New England Journal of Medicine* 360:1500–1508.
- [14] Zingaretti, M.C., Crosta, F., Vitali, A., Guerrieri, M., Frontini, A., et al., 2009. The presence of UCP1 demonstrates that metabolically active adipose tissue in the neck of adult humans truly represents brown adipose tissue. *FASEB Journal* 23:3113–3120.
- [15] Wu, J., Boström, P., Sparks, L.M., Ye, L., Choi, J.H., et al., 2012. Beige adipocytes are a distinct type of thermogenic fat cell in mouse and human. *Cell* 150:366–376.
- [16] Waldén, T.B., Hansen, I.R., Timmons, J.A., Cannon, B., Nedergaard, J., 2012. Recruited vs. nonrecruited molecular signatures of brown, “brite,” and white adipose tissues. *American Journal of Physiology. Endocrinology and Metabolism* 302:E19–E31.
- [17] Himms-Hagen, J., Melnyk, A., Zingaretti, M.C., Ceresi, E., Barbatelli, G., Cinti, S., 2000. Multilocular fat cells in WAT of CL-316243-treated rats derive directly from white adipocytes. *American Journal of Physiology. Cell physiology* 279:C670–C681.
- [18] Cao, W., Medvedev, A.V., Daniel, K.W., Collins, S., 2001. beta-Adrenergic activation of p38 MAP kinase in adipocytes: cAMP induction of the uncoupling protein 1 (UCP1) gene requires p38 MAP kinase. *Journal of Biological Chemistry* 276:27077–27082.
- [19] Bachman, E.S., Dhillon, H., Zhang, C.Y., Cinti, S., Bianco, A.C., et al., 2002. betaAR signaling required for diet-induced thermogenesis and obesity resistance. *Science* 297:843–845.
- [20] Rehnmark, S., Né Chad, M., Herron, D., Cannon, B., Nedergaard, J., 1990. Alpha- and beta-adrenergic induction of the expression of the uncoupling protein thermogenin in brown adipocytes differentiated in culture. *Journal of Biological Chemistry* 265:16464–16471.
- [21] Cypess, A.M., Weiner, L.S., Roberts-Toler, C., Franquet, E.E., Kessler, S.H., et al., 2015. Activation of human brown adipose tissue by a  $\beta$ 3-adrenergic receptor agonist. *Cell Metabolism* 21:33–38.
- [22] Jespersen, N.Z., Larsen, T.J., Peijs, L., Dugaard, S., Homøe, P., et al., 2013. A classical brown adipose tissue mRNA signature partly overlaps with brite in the supraclavicular region of adult humans. *Cell Metabolism* 17: 798–805.
- [23] Yoneshiro, T., Saito, M., 2014. Activation and recruitment of brown adipose tissue as anti-obesity regimens in humans. *Annals of Medicine* 5:1–9.
- [24] Cypess, A.M., Chen, Y.C., Sze, C., Wang, K., English, J., et al., 2012. Cold but not sympathomimetics activates human brown adipose tissue in vivo. *Proceedings of the National Academy of Sciences of the United States of America* 109:10001–10005.
- [25] Broeders, E., Bouvy, N.D., van Marken Lichtenbelt, W.D., 2015. Endogenous ways to stimulate brown adipose tissue in humans. *Annals of Medicine* 47:123–132.
- [26] Cannon, B., Nedergaard, J., 2011. Nonshivering thermogenesis and its adequate measurement in metabolic studies. *Journal of Experimental Biology* 214:242–253.
- [27] Speakman, J.R., Keijer, J., 2012. Not so hot: optimal housing temperatures for mice to mimic the thermal environment of humans. *Molecular Metabolism* 2: 5–9.

- [28] Sanghez, V., Razzoli, M., Carobbio, S., Campbell, M., McCallum, J., et al., 2013. Psychosocial stress induces hyperphagia and exacerbates diet-induced insulin resistance and the manifestations of the metabolic syndrome. *Psychoneuroendocrinology* 38:2933–2942.
- [29] Epel, E., Jimenez, S., Brownell, K., Stroud, L., Stoney, C., Niaura, R., 2004. Are stress eaters at risk for the metabolic syndrome? *Annals of the New York Academy of Sciences* 1032:208–210.
- [30] Kivimäki, M., Head, J., Ferrie, J.E., Shipley, M.J., Brunner, E., et al., 2006. Work stress, weight gain and weight loss: evidence for bidirectional effects of job strain on body mass index in the Whitehall II study. *International Journal of Obesity* 30:982–987.
- [31] Bartolomucci, A., Cabassi, A., Govoni, P., Ceresini, G., Cero, C., et al., 2009. Metabolic consequences and vulnerability to diet-induced obesity in male mice under chronic social stress. *PLoS One* 4:e4331.
- [32] Razzoli, M., Sanghez, V., Bartolomucci, A., 2015. Chronic subordination stress induces hyperphagia and disrupts eating behavior in mice modeling binge-eating-like disorder. *Frontiers in Nutrition* 1 pii: 00030.
- [33] Razzoli, M., Karsten, C., Yoder, J.M., Bartolomucci, A., Engeland, W.C., 2014. Chronic subordination stress phase advances adrenal and anterior pituitary clock gene rhythms. *American Journal of Physiology. Regulatory, Integrative and Comparative Physiology* 307:R198–R205.
- [34] Tschöp, M.H., Speakman, J.R., Arch, J.R., Auwerx, J., Brüning, J.C., et al., 2011. A guide to analysis of mouse energy metabolism. *Nature Methods* 9:57–63.
- [35] Hu, H.H., Perkins, T.G., Chia, J.M., Gilsanz, V., 2013. Characterization of human brown adipose tissue by chemical-shift water-fat MRI. *American Journal Roentgenology* 200:177–183.
- [36] Hu, H.H., Smith Jr., D.L., Nayak, K.S., Goran, M.I., Nagy, T.R., 2010. Identification of brown adipose tissue in mice with fat-water IDEAL-MRI. *Journal of Magnetic Resonance Imaging* 31:1195–1202.
- [37] Bolan, P.J., Puranik, A., Osborn, J.W., Razzoli, M., Bartolomucci, A., et al., 2014. Whole-body imaging of adipose tissues in mouse at 9.4T. In: *Proceedings of the 22nd Annual Meeting ISMRM, Milan, 2014*. p. 3615.
- [38] Pfaffl, M.W., Tichopad, A., Prgomet, C., Neuvians, T.P., 2004. Determination of stable housekeeping genes, differentially regulated target genes and sample integrity: BestKeeper—Excel-based tool using pair-wise correlations. *Biotechnology Letters* 26:509–515.
- [39] Medina, I., Carbonell, J., Pulido, L., Madeira, S.C., Goetz, S., et al., 2010. Babelomics: an integrative platform for the analysis of transcriptomics, proteomics and genomic data with advanced functional profiling. *Nucleic Acids Research* 38:W210–W213.
- [40] Al Shahrour, F., Arbiza, L., Dopazo, H., et al., 2007. From genes to functional classes in the study of biological systems. *BMC Bioinformatics* 8:114.
- [41] Vitali, A., Murano, I., Zingaretti, M.C., Frontini, A., Ricquier, D., Cinti, S., 2012. The adipose organ of obesity-prone C57BL/6J mice is composed of mixed white and brown adipocytes. *Journal of Lipid Research* 53:619–629.
- [42] Morrison, S.F., Madden, C.J., Tupone, D., 2014. Central neural regulation of brown adipose tissue thermogenesis and energy expenditure. *Cell Metabolism* 19:741–756.
- [43] Barbatelli, G., Murano, I., Madsen, L., Hao, Q., Jimenez, M., et al., 2010. The emergence of cold-induced brown adipocytes in mouse white fat depots is determined predominantly by white to brown adipocyte transdifferentiation. *American Journal of Physiology. Endocrinology and Metabolism* 298:E1244–E1253.
- [44] Nedergaard, J., Cannon, B., 2014. The browning of white adipose tissue: some burning issues. *Cell Metabolism* 20:396–407.
- [45] Kataoka, N., Hioki, H., Kaneko, T., Nakamura, K., 2014. Psychological stress activates a dorsomedial hypothalamus-medullary raphe circuit driving brown adipose tissue thermogenesis and hyperthermia. *Cell Metabolism* 20:346–358.
- [46] Smorlesi, A., Frontini, A., Giordano, A., Cinti, S., 2012. The adipose organ: white-brown adipocyte plasticity and metabolic inflammation. *Obesity Review* 13(Suppl. 2):83–96.
- [47] Frontini, A., Cinti, S., 2010. Distribution and development of brown adipocytes in the murine and human adipose organ. *Cell Metabolism* 11:253–256.
- [48] Seale, P., Bjork, B., Yang, W., Kajimura, S., Chin, S., et al., 2008. PRDM16 controls a brown fat/skeletal muscle switch. *Nature* 454:961–967.
- [49] Timmons, J.A., Wennmalm, K., Larsson, O., Walden, T.B., Lassmann, T., et al., 2007. Myogenic gene expression signature establishes that brown and white adipocytes originate from distinct cell lineages. *Proceedings of the National Academy of Sciences of the United States of America* 104:4401–4406.
- [50] Nedergaard, J., Cannon, B., 2013. UCP1 mRNA does not produce heat. *Biochimica et Biophysica Acta* 1831:943–949.
- [51] Ye, L., Wu, J., Cohen, P., Kazak, L., Khandekar, M.J., et al., 2013. Fat cells directly sense temperature to activate thermogenesis. *Proceedings of the National Academy of Sciences of the United States of America* 110:12480–12485.
- [52] Kikuchi-Utsumi, K., Kikuchi-Utsumi, M., Cannon, B., Nedergaard, J., 1997. Differential regulation of the expression of alpha1-adrenergic receptor subtype genes in brown adipose tissue. *Biochemical Journal* 322:417–424.
- [53] Alvarez-Llamas, G., Szalowska, E., de Vries, M.P., Weening, D., Landman, K., et al., 2007. Characterization of the human visceral adipose tissue secretome. *Molecular & Cellular Proteomics* 6:589–600.
- [54] Burnstock, G., 2007. Physiology and pathophysiology of purinergic neurotransmission. *Physiological Reviews* 87:659–797.
- [55] De Mattei, R., Ricquier, D., Cinti, S., 1999. TH-, NPY-, SP-, and CGRP-immunoreactive nerves in interscapular brown adipose tissue of adult rats acclimated at different temperatures: an immunohistochemical study. *Journal of Neurocytology* 27:877–886.
- [56] Bartness, T.J., Liu, Y., Shrestha, Y.B., Ryu, V., 2014. Neural innervation of white adipose tissue and the control of lipolysis. *Frontiers in Neuroendocrinology* 35:473–493.
- [57] Ussar, S., Lee, K.Y., Dankel, S.N., Boucher, J., Haering, M.F., et al., 2014. ASC-1, PAT2, and P2RX5 are cell surface markers for white, beige, and brown adipocytes. *Science Translational Medicine* 6:247ra103.
- [58] Gnad, T., Scheibler, S., von Kügelgen, I., Scheele, C., Kilić, A., et al., 2014. Adenosine activates brown adipose tissue and recruits beige adipocytes via A2A receptors. *Nature* 516:395–399.
- [59] Sawada, K., Echigo, N., Juge, N., Miyaji, T., Otsuka, M., et al., 2008. Identification of a vesicular nucleotide transporter. *Proceedings of the National Academy of Sciences of the United States of America* 105:5683–5686.
- [60] Hiasa, M., Togawa, N., Moriyama, Y., 2014. Vesicular nucleotide transport: a brief history and the vesicular nucleotide transporter as a target for drug development. *Current Pharmaceutical Design* 20:2745–2749.
- [61] Lee, S.C., Vielhauer, N.S., Leaver, E.V., Pappone, P.A., 2005. Differential regulation of ca(2+) signaling and membrane trafficking by multiple p2 receptors in brown adipocytes. *Journal of Membrane Biology* 207:131–142.
- [62] Krishnan, V., Han, M.H., Graham, D.L., Berton, O., Renthal, W., et al., 2007. Molecular adaptations underlying susceptibility and resistance to social defeat in brain reward regions. *Cell* 131:391–404.
- [63] Nasca, C., Bigio, B., Zelli, D., Nicoletti, F., McEwen, B.S., 2014. Mind the gap: glucocorticoids modulate hippocampal glutamate tone underlying individual differences in stress susceptibility. *Molecular Psychiatry* 20:755–763.
- [64] Marniemi, J., Kronholm, E., Aunola, S., Toikka, T., Mattlar, C.E., et al., 2002. High stress-emotional reaction in the obese co-twin visceral fat and psychosocial stress in identical twins discordant for obesity. *Journal of Internal Medicine* 251:35–43.
- [65] Rosmond, R., Dallman, M.F., Björntorp, P., 1988. Stress-related cortisol secretion in men: relationships with abdominal obesity and endocrine, metabolic and hemodynamic abnormalities. *Journal of Clinical Endocrinology & Metabolism* 83:1853–1859.
- [66] Shively, C.A., Register, T.C., Clarkson, T.B., 2009. Social stress, visceral obesity, and coronary artery atherosclerosis in female primates. *Obesity (Silver Spring)* 17:1513–1520.

- [67] Brunner, E.J., Chandola, T., Marmot, M.G., 2007. Prospective effect of job strain on general and central obesity in the Whitehall II study. *American Journal of Epidemiology* 165:828–837.
- [68] Harris, R.B., 2015. Chronic and acute effects of stress on energy balance: are there appropriate animal models? *American Journal of Physiology. Regulatory, Integrative and Comparative Physiology* 308:R250–R265.
- [69] Razzoli, M., Cero, C., Bartolomucci, A., 2015. How does stress affects energy balance? Recent advances in physiology and neurobehavioral genetics. In: Tucci, V. (Ed.), *Phenotyping behaviour and cognition. Towards a cutting-edge neurobehavioural genetics. Wiley Book series* [in press].
- [70] Koolhaas, J.M., Bartolomucci, A., Buwalda, B., de Boer, S.F., Flügge, G., et al., 2011. Stress revisited: a critical evaluation of the stress concept. *Neuroscience & Biobehavioral Reviews* 35:1291–1301.
- [71] Sapolsky, R.M., 2005. The influence of social hierarchy on primate health. *Science* 308:648–652.
- [72] Patterson, Z.R., Khazall, R., Mackay, H., Anisman, H., Abizaid, A., 2013. Central ghrelin signaling mediates the metabolic response of C57BL/6 male mice to chronic social defeat stress. *Endocrinology* 154:1080–1091.
- [73] Bartolomucci, A., Carola, V., Pascucci, T., Puglisi-Allegra, S., Cabib, S., et al., 2010. Increased vulnerability to psychosocial stress in heterozygous serotonin transporter knockout mice. *Disease Models & Mechanisms* 3:459–470.
- [74] Chuang, J.C., Krishnan, V., Yu, H.G., Mason, B., Cui, H., et al., 2010. A beta3-adrenergic-leptin-melanocortin circuit regulates behavioral and metabolic changes induced by chronic stress. *Biological Psychiatry* 67:1075–1082.
- [75] Bartelt, A., Bruns, O.T., Reimer, R., Hohenberg, H., Ittrich, H., et al., 2011. Brown adipose tissue activity controls triglyceride clearance. *Nature Medicine* 17:200–205.
- [76] Kir, S., White, J.P., Kleiner, S., Kazak, L., Cohen, P., et al., 2014. Tumor-derived PTH-related protein triggers adipose tissue browning and cancer cachexia. *Nature* 513:100–104.
- [77] Thomas, S.A., Palmiter, R.D., 1997. Thermoregulatory and metabolic phenotypes of mice lacking noradrenaline and adrenaline. *Nature* 387:94–97.
- [78] Sidman, R.L., Fawcett, D.W., 1954. The effect of peripheral nerve section on some metabolic responses of brown adipose tissue in mice. *Anatomical Record* 118:487–507.
- [79] Lee, Y.H., Petkova, A.P., Konkar, A.A., Granneman, J.G., 2015. Cellular origins of cold-induced brown adipocytes in adult mice. *FASEB Journal* 29:286–299.
- [80] Wang, Q.A., Tao, C., Gupta, R.K., Scherer, P.E., 2013. Tracking adipogenesis during white adipose tissue development, expansion and regeneration. *Nature Medicine* 19:1338–1344.
- [81] Gourine, A.V., Wood, J.D., Burnstock, G., 2009. Purinergic signalling in autonomic control. *Trends in Neurosciences* 32:241–248.
- [82] Sakamoto, S., Miyaji, T., Hiasa, M., Ichikawa, R., Uematsu, A., et al., 2014. Impairment of vesicular ATP release affects glucose metabolism and increases insulin sensitivity. *Scientific Reports* 4:6689.